Minimum superlattice thermal conductivity from molecular dynamics

Yunfei Chen*
Department of Mechanical Engineering and China Education Council Key Laboratory of MEMS, Southeast University, Nanjing, 210096, People's Republic of China

Deyu Li
Department of Mechanical Engineering, Vanderbilt University, Nashville, Tennessee 37235-1592, USA

Jennifer R. Lukes
Department of Mechanical Engineering and Applied Mechanics, University of Pennsylvania, Philadelphia, Pennsylvania 19104-6315, USA

Zhonghua Ni and Minhua Chen
Department of Mechanical Engineering and China Education Council Key Laboratory of MEMS, Southeast University, Nanjing, 210096, People's Republic of China

(Received 30 June 2005; revised manuscript received 27 July 2005; published 7 November 2005)

The dependence of superlattice thermal conductivity on period length is investigated by molecular dynamics simulation. For perfectly lattice matched superlattices, a minimum is observed when the period length is of the order of the effective phonon mean free path. As temperature decreases and interatomic potential strength increases, the position of the minimum shifts to larger period lengths. The depth of the minimum is strongly enhanced as mass and interatomic potential ratios of the constituent materials increase. The simulation results are consistent with phonon transmission coefficient calculations, which indicate increased stop bandwidth and thus strongly enhanced Bragg scattering for the same conditions under which strong reductions in thermal conductivity are found. When nonideal interfaces are created by introducing a 4% lattice mismatch, the minimum disappears and thermal conductivity increases monotonically with period length. This result may explain why minimum thermal conductivity has not been observed in a large number of experimental studies.

DOI: 10.1103/PhysRevB.72.174302 PACS number(s): 66.70.+f, 68.65.Cd

Understanding the thermal conductivity of superlattice (SL) structures is of great importance for improving the performance of thermoelectric energy converters and optoelectronic devices. Over the past two decades, numerous experimental and theoretical studies have been carried out to investigate the thermal transport process in various kinds of SLs.[1–6] Results from these studies provide insight into phonon transport in SL structures but also pose puzzling problems. This arises from the complicated physics of phonon transport in SLs. Depending on the SL materials, interface properties, and period length, the transport can be dominated by either the wave or the particle nature of phonons. In addition, phonons are broadband with frequencies spanning the Brillouin zone, which makes the transport more complicated.

One interesting problem is the minimum thermal conductivity predicted by several theoretical analyses and observed by a few experimental studies. Based on kinetic theory, the phonon thermal conductivity can be derived as $k=\frac{1}{3}Cvl$, where C is the specific heat per unit volume, v is the sound velocity, and l is the phonon mean free path. As the interface density per unit length increases, thermal conductivity is reduced because the phonon mean free path is limited to the layer thickness. This trend has been observed in many experimental investigations on different SLs such as those made of Si/Ge and Si/SiGe.[6–8] Nonetheless, with a further decrease in layer thickness, the reverse trend is sometimes observed, i.e., the thermal conductivities of shorter period length SLs increase as the layer thickness decreases. This cannot be directly explained by the particle treatment of phonons based on the Boltzmann transport theory. Several attempts have been carried out to explain this phenomenon based on the wave nature of phonons. It has been argued that due to coherent backscattering of phonon waves at the SL interfaces, the phonon spectrum is modified and a series of minibands appear, which leads to the phonon localizationlike behavior in SL structures and a minimum in thermal conductivity at a particular period length. Simkin and Mahan[9] used a lattice dynamics model to show that the minimum thermal conductivity is due to miniband formation and occurs at the crossover between the particle and wave interference regimes. They predicted that the minimum thermal conductivity should be observed for most SLs since at room temperature, in most solids, anharmonic scattering limits the phonon mean free path to values in the range of 10–100 lattice constants, which covers the typical layer thickness in SLs. However, in their model, the phonon mean free path was assumed to be constant for SLs with different period lengths, which did not consider the possible limitation of interface scattering on phonon mean free path. Indeed, only a few experiments[1,10] have observed the minimum thermal conductivity in SL structures, while most experiments show a monotonically decreasing thermal conductivity as the period length is reduced.

An explicit explanation of if and when the minimum thermal conductivity exists is key to understanding the physics of phonon transport in superlattices. Molecular dynamics

(MD) has been proved to be a powerful tool for modeling phonon transport in SLs and for providing detailed information on the effects of various quantities such as lattice parameter and mass of the constituent materials. Volz *et al.*[11] used molecular dynamics to simulate heat transfer in strained Si/Ge multilayered structures. A conjugate gradient method was introduced to minimize the potential energy in order to relax the elastic strain on the alternating layers. Simulation results predicted a monotonic increase of SL thermal conductivity with layer thickness. Daly *et al.*[12] used a highly simplified model to simulate the effects of smooth and rough interfaces on the lattice thermal conductivity of GaAs/AlAs SLs. For smooth interfaces, they observed a minimum thermal conductivity at a SL layer thickness of about eight monolayers. They introduced roughness by randomly assigning the mass of each atom at the interface to be the mass of either an "effective" GaAs atom or an "effective" AlAs atom. The results demonstrated that the rough interface further reduced lattice thermal conductivity and eliminated the minimum thermal conductivity.

Here we report a nonequilibrium molecular dynamics (NEMD) simulation on a model SL structure consisting of alternating layers of two different materials. By exploring the effects of various parameters such as lattice constant, period length, phonon mean free path, interatomic potential strength, and atomic mass of the alternating layers, we try to explain the physics of the minimum thermal conductivity of SLs. The results show that a minimum thermal conductivity will occur if the phonon mean free path is comparable to or longer than the period length and the lattice constants of the alternating layers are very close to each other. If the lattice constants of the two alternating layers are different, lattice mismatch will lead to diffuse scattering and eliminate the minimum thermal conductivity. The interatomic potential strength difference and the mass ratio of the alternating layers affect the value of the minimum thermal conductivity, providing insights for designing SL structures for tunable thermal properties.

The model system was constructed of face-centered-cubic unit cells (UCs) oriented in the [100] direction. The Lennard-Jones (LJ) potential is used to represent the interaction between atoms in the model system,

TABLE I. Physical parameters for Fig. 1.

Atomic mass ratio of A and B	$\alpha_A=1$,	$\alpha_B=1.2$
Length scale ratio of A and B	$\beta_A=1$,	$\beta_B=1$
Interatomic strength ratio of A and B	Case I	$\gamma_A=1$, $\gamma_B=1$
	Case II	$\gamma_A=5$, $\gamma_B=5$
	Case III	$\gamma_A=10$, $\gamma_B=10$
Phonon mean free path of bulk A	Case I	1.22 nm (2.3 UC)
	Case II	6.91 nm (13 UC)
	Case III	19.96 nm (37.5 UC)

$$V(r_{ij}) = 4\varepsilon\left\{\left(\frac{\sigma}{r_{ij}}\right)^{12} - \left(\frac{\sigma}{r_{ij}}\right)^{6}\right\} \tag{1}$$

where r_{ij} is the distance between atoms i and j, ε is the well depth of the potential and σ represents the equilibrium separation distance. In order to explore the effects of material selection on the SL thermal conductivity, different well depth and equilibrium separation distances were explored in the simulation. Three dimensionless physical parameters α, β, and γ are introduced as

$$\alpha = \frac{m_i}{m_0}, \quad \beta = \frac{\sigma_i}{\sigma_0}, \quad \gamma = \frac{\varepsilon_i}{\varepsilon_0} \tag{2}$$

where $m_0, \sigma_0, \varepsilon_0$ stand for the atomic mass, the equilibrium separation distance, and the well depth in the LJ potential for solid argon at 0 K. The variables with subscript i stand for the physical parameters of the model SL. Subscripts A and B are used to denote the alternating layers. For example, α_A is the mass ratio of the atoms in layer A to the reference mass. The arithmetic mean coefficients are introduced to describe the interactions between the atoms in the adjacent layers, following Ref. 13:

$$\varepsilon_{AB} = \sqrt{\varepsilon_A \times \varepsilon_B}, \quad \sigma_{AB} = (\sigma_A + \sigma_B)/2. \tag{3}$$

The simulation domain consists of a hot bath with a high constant temperature, T_H, at one end, and a cold bath with a low constant temperature, T_L, at the other end, with alternat-

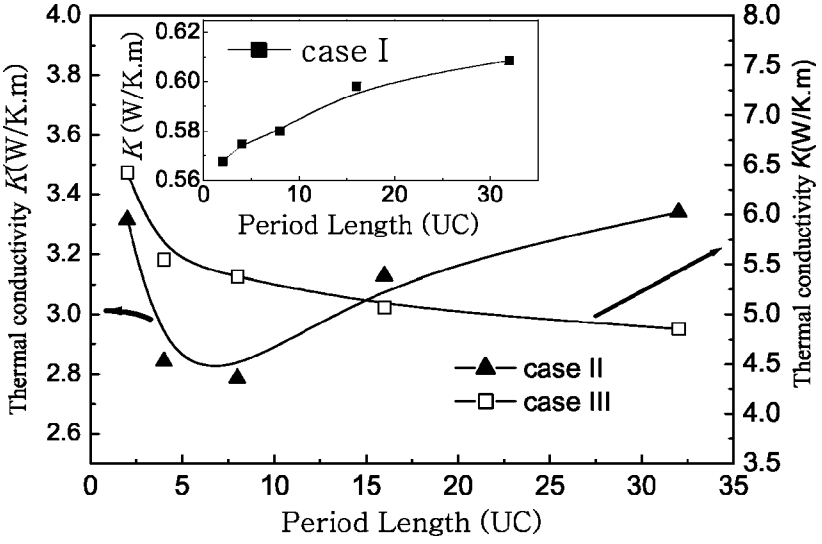

FIG. 1. Thermal conductivity of SL (40 K) versus period length for different well depths. The ratios of lattice constants and masses in B and A are 1 and 1.2, respectively.

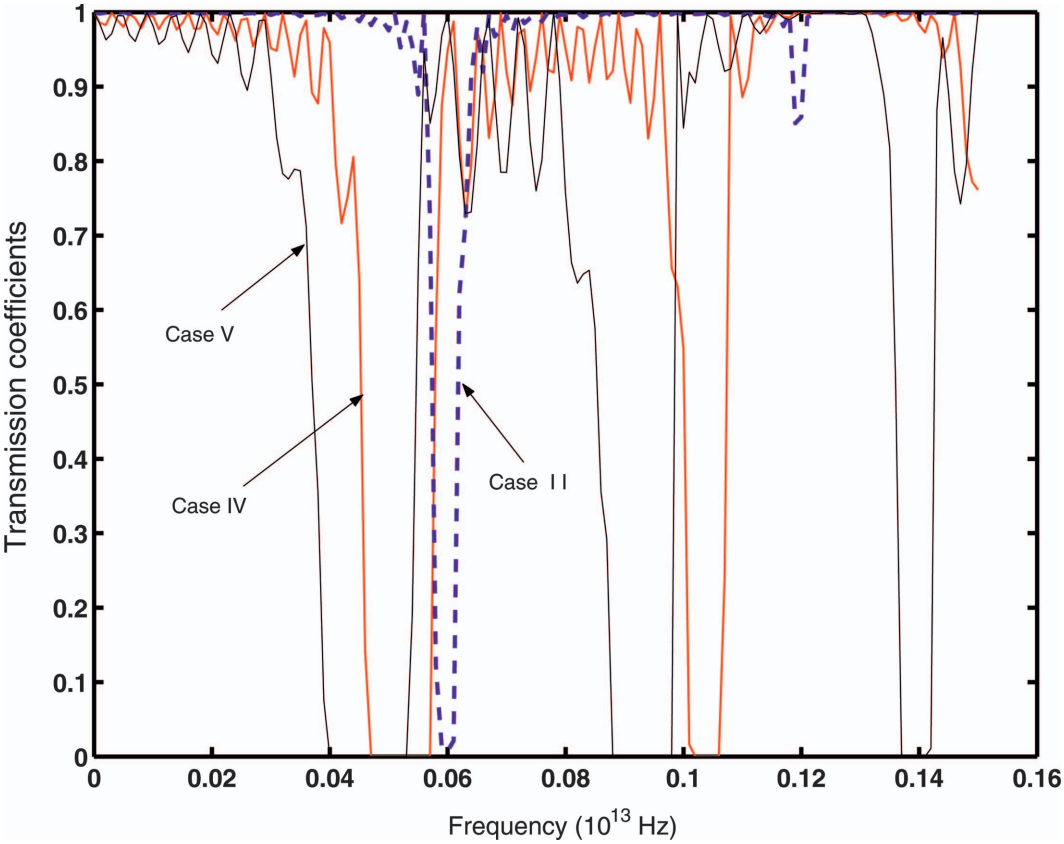

FIG. 2. (Color) Phonon transmission coefficients at 40 K for SL with different mass and well depth ratios between the two alternating layers. The parameters are listed in Table II.

ing layers of materials A and B in between. A constant heat flux was added to the hot bath and the same amount of heat flux was subtracted from the cold bath. This way, heat flux was introduced into the simulation domain and a temperature gradient was set up along the heat flux direction. From the heat flux J and the temperature gradient, the thermal conductivity of the SL can be calculated from the Fourier law

$$K = \frac{-J}{A \nabla T} \tag{4}$$

where A is the cross sectional area and ∇T is the temperature gradient. Periodic boundary conditions were used in the directions perpendicular to the heat flux. More details of the simulation can be found in Refs. 14–16.

Finite size in MD simulation may introduce artificial effects. For NEMD, phonon scattering at the hot and cold bath boundaries may lead to shorter phonon mean free path and smaller thermal conductivity. The effective phonon mean free path is related to the simulation domain length, l_z, and a simple formula was given by Schelling[17] to estimate the effective phonon mean free path l_{eff},

$$\frac{1}{l_{eff}} = \frac{1}{l_\infty} + \frac{2}{l_z} \tag{5}$$

where l_∞ is the phonon mean free path in an infinite system. l_{eff} approaches l_∞ as the simulation domain increases. If the particle treatment of phonons is valid, l_∞ and the intrinsic thermal conductivity can be derived from a plot of $1/\kappa$ vs $1/l_z$, which should be linear. Following this procedure, the intrinsic thermal conductivity of an infinite system can be obtained by extrapolating to $1/l_z=0$. This way, the finite simulation domain effect can be removed. This procedure

TABLE II. Physical parameters for Figs. 2–4.

	Case II	Case IV	Case V
Atomic mass ratio of A and B	$\alpha_A=1,\ \alpha_B=1.2$	$\alpha_A=1,\ \alpha_B=2$	$\alpha_A=1,\ \alpha_B=1$
Length scale ratio of A and B	$\beta_A=1,\ \beta_B=1$	$\beta_A=1,\ \beta_B=1$	$\beta_A=1,\ \beta_B=1$
Interatomic strength ratio of A and B	$\gamma_A=5,\ \gamma_B=5$	$\gamma_A=5,\ \gamma_B=5$	$\gamma_A=2,\ \gamma_B=5$
The acoustic impedance ratio of layer B to layer A	$Z_B/Z_A=1.095$	$Z_B/Z_A=1.414$	$Z_B/Z_A=1.581$

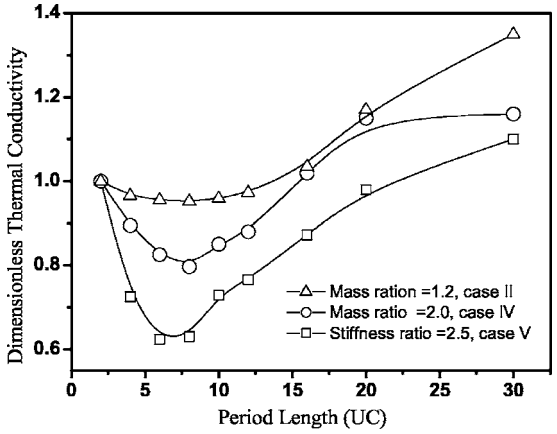

FIG. 3. Superlattice thermal conductivity for different mass ratios and interatomic potential strength. The parameters are listed in Table II.

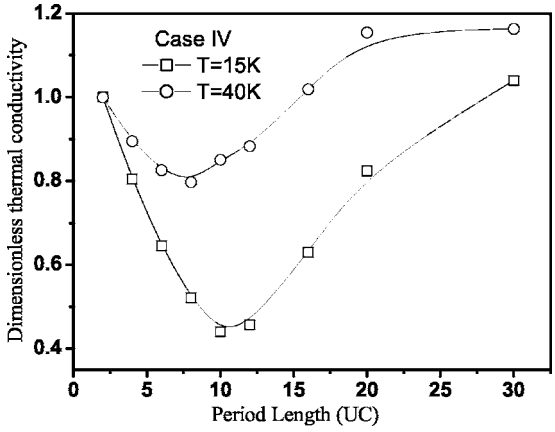

FIG. 4. Period length dependence of thermal conductivity at different temperatures.

was adopted to model those SLs with larger period length, since for longer period, the phonon-phonon scattering within each period will destroy the coherence and phonon transport can be treated as particle transport. If the period length is smaller, the above described treatment is not adopted since the wave nature of phonons may be important. Instead, the simulation domain size was increased until thermal conductivity was no longer dependent on the total length. We found that a total length of 128 UCs is enough to make the finite size effect marginal for SLs with period length less than 8 UCs.

To explore the effect of phonon mean free path, we assign the SL with parameters as listed in Table I. The phonon mean free path is evaluated from the extrapolation method described above. Figure 1 shows the thermal conductivity of SLs at 40 K versus period length. The period length ranges from 2 UCs to 32 UCs. The two materials *A* and *B* have the same equilibrium distance in the LJ potential, which means that they have the same lattice constants and the two materials have ideal interfaces. The only difference between the two materials is their atomic masses. The atomic mass ratio of *B* to *A* is 1.2. The results show that if the strength of the LJ interatomic potential is the same as that of solid argon, the lattice thermal conductivity increases monotonically with the period length. However, if the interatomic potential strength is increased, the thermal conductivity will first decrease with increasing period length, then increase, yielding a minimum thermal conductivity in simulation case II. As shown in Table I, larger well depths correspond to longer phonon mean free paths. Case II shows that the value of the thermal conductivity reaches a minimum when the period length is about the same as the phonon mean free path in the bulk materials *A* or *B*. As the phonon mean free path of the bulk materials *A* and *B* further increases, the minimum shifts to longer period lengths and cannot be observed for case III in Fig. 1. This result supports Simkin and Mahan's lattice dynamics model, i.e., if the layer thickness is smaller than the phonon mean free path, SL thermal conductivity will show a minimum with respect to period length.

If phonons are treated as waves, the thermal conductivity reduction in SLs arises from two reasons. Both are due to band folding or miniband formation. When zone folding occurs, the overall phonon group velocity decreases with increasing period length, leading to a decrease of thermal conductivity as the period length increases. In addition, the zone folding leads to stop bands in the phonon dispersions for SLs. These stop bands filter the phonons with energies in the stop bands and prevent their transport through the SL. The phonon transmission coefficients can be calculated with transfer matrix techniques.[18–20] Figure 2 shows the phonon transmission coefficients for SLs of different masses and different well depths. The physical parameters are listed in Table II. In Fig. 2, the phonon transmission coefficients for cases II, case IV and V are depicted together to compare the width of the stop bands. The acoustic impedance difference between the two alternating layers, which is computed from the mass and the phonon group velocity, is the smallest for case II, larger for case IV, and the largest for case V. The calculated results demonstrate that the width of the stop band increases with increasing acoustic impedance mismatch. Wider stop bands indicate enhanced phonon reflection at the interface and reduced energy transport.

Figure 3 shows the thermal conductivity versus period length for the three cases listed in Table II at 40 K. The thermal conductivities in Fig. 3 are normalized with the ther-

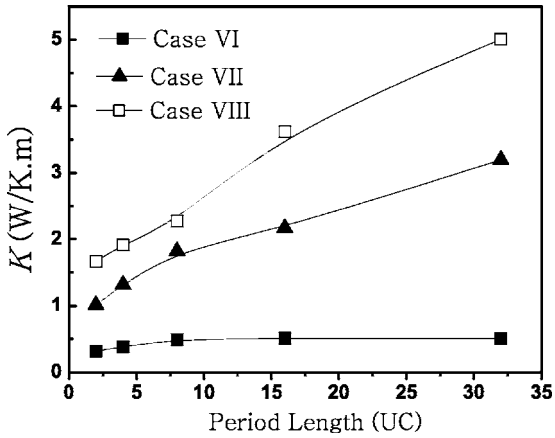

FIG. 5. Relationship between thermal conductivity and period length for 4% lattice mismatch.

TABLE III. Physical parameters for Fig. 5.

Atom mass of material A and B	$\alpha_A=1$,	$\alpha_B=1.2$
Length scale in LJ potential for material A and B	$\beta_A=1$,	$\beta_B=1.04$
Well depth in LJ potential for material A and B	Case VI	$\gamma_A=1$, $\gamma_B=1$
	Case VII	$\gamma_A=5$, $\gamma_B=5$
	Case VIII	$\gamma_A=10$, $\gamma_B=10$

mal conductivity values for SLs with the shortest period length, $L_p=2$ UCs. The largest thermal conductivity reduction occurs for case V. As demonstrated in Fig. 2, the SL for case V has the widest stop bands due to its largest acoustic impedance mismatch between the two alternating layers.

In order to verify the above argument, more simulations with different parameters were carried out at different temperatures. Figure 4 shows the SL thermal conductivity at temperatures $T=40$ K and 15 K. As the simulation temperature is below the Debye temperature of Ar (92 K), quantum modification should be introduced to correct both the MD temperature and the thermal conductivity. However, it has been suggested[16] that the classical MD model could give acceptable prediction for lattice thermal conductivity as long as the temperature is higher than 10 K for Ar. The physical parameters used for both cases in Fig. 4 are the same as that of case IV in Table II. Similarly to Fig. 3, the results are normalized with the thermal conductivity values for SLs with the shortest period length, $L_p=2$ UCs. The interesting result is that the valley depth in the curve for thermal conductivity at 15 K is far deeper than that at 40 K. The minimum thermal conductivity at 40 K is about 80% of the reference thermal conductivity value while the one at 15 K is about 45% of the reference value. In addition, the valley position shifts slightly from a period length of about 8 UC to a period length of about 11 UC. For lower temperature, the U scattering process becomes weaker and contributes less resistance to phonon transport, leading to a longer intrinsic phonon mean free path and a higher thermal conductivity. The weaker U scattering process makes the zone folding effects more prominent in the total thermal resistance, leading to a larger percentage thermal conductivity reduction. Comparison between Figs. 3 and 4 indicates that the wider the stop bands, the stronger the thermal conductivity reduction due to zone folding.

Although the present work and previous more simplified work predicted the minimum thermal conductivity, it has not been widely observed in experimental measurements. Note that all the simulations above are for perfectly lattice matched SLs, i.e., the two alternating layers have the same lattice constant. In reality, the lattice constants of the two alternating layers almost always have some difference. To study the effects of lattice constant, we set the lattice constant of layer B to be 4% larger than that of layer A. Figure 5 shows the thermal conductivity versus period length for SL structures with parameters as given in Table III. It is clear from Fig. 5 that if the lattice constants are different by 4%, the minimum thermal conductivity disappears and the thermal conductivity decreases monotonically with decreasing period length. We believe that the lattice mismatch between the two materials destroys the Bragg reflection conditions and the phonons striking the interfaces will be diffusely scattered and lose coherency. In this case, the phonon mean free path is limited by the layer thickness and the particle treatment is valid. So to observe the minimum thermal conductivity in experiments, the difference between the lattice constants of the two alternating layers must be as small as possible.

In summary, we used a nonequilibrium molecular dynamics simulation with the Lennard-Jones potential to investigate the minimum thermal conductivity of superlattices. Our results show that the minimum thermal conductivity occurs if the phonon mean free path is comparable to or larger than the period length and the lattice constants of the alternating layers are very close to each other. Comparison between transmission coefficient calculations and the thermal conductivity results indicates that larger stop bandwidth leads to stronger thermal conductivity reduction. Lattice mismatch leads to diffuse phonon scattering and destroys the Bragg reflection conditions, which eliminate the minimum thermal conductivity. The thermal conductivity decreases monotonically with decreasing period length if the lattice constants of the two alternating layers differ by 4%.

The authors would like to acknowledge financial support from the National Basic Research program of China (2006CB300404) and the Natural Science Foundation of China (50276011, 50275026, 50475077) and partial support from Jiangsu Province Nature Science Foundation (BK2002060).

*Electronic mail: yunfeichen@seu.edu.cn

[1] R. Venkatasubramanian, Phys. Rev. B **61**, 3091 (2000).

[2] T. Yao, Appl. Phys. Lett. **51**, 1798 (1987).

[3] W. S. Capinski, M. Cardona, and D. S. Katzer, Physica B **219**, 699 (1996).

[4] G. Chen, C. L. Tien, X. Wu, and J. S. Smith, J. Heat Transfer **116**, 325 (1994).

[5] T. Borca-Tasciuc, W. Liu, J. L. Liu, T. Zeng, D. W. Song, C. D. Moore, G. Chen, K. L. Wang, M. S. Goorsky, T. Radetic, R. Gronsky, T. Koga, and M. S. Dresselhaus, Superlattices

Microstruct. **28**, 199 (2000).
[6] S. M. Lee, David G. Cahill, and R. Venkatasubramanian, Appl. Phys. Lett. **70**, 2957 (1997).
[7] S. T. Huxtable, A. Abramson, A. Majumdar, C.-L. Tien, G. Zeng, C. LaBounty, A. Shakouri, J. E. Bowers, and E. Croke, Appl. Phys. Lett. **80**, 1737 (2002).
[8] W. S. Capinski, H. J. Maris, T. Ruf, M. Cardona, K. Ploog, and D. S. Katzer, Phys. Rev. B **59**, 8105 (1999).
[9] M. V. Simkin and G. D. Mahan, Phys. Rev. Lett. **84**, 927 (2000).
[10] S. Chakraborty, C. A. Kleint, A. Heinrich, C. M. Schneider, and J. Schumann, M. Falke, and S. Teichert, Appl. Phys. Lett. **83**, 4184 (2003).
[11] S. Volz, J. B. Saulnier, G. Chen, and P. Beauchamp, High Temp. - High Press. **32**, 709 (2000).
[12] B. C. Daly, H. J. Maris, K. Imamura, and S. Tamura, Phys. Rev. B **66**, 024301 (2002).
[13] S. Volz, J. B. Saulnier, G. Chen, and P. Beauchamp, Microelectron. J. **31**, 815 (2000).
[14] C. J. Twu and J. R. Ho, Phys. Rev. B **67**, 205422 (2003).
[15] J. R. Lukes, D. Li, X.-G. Liang, and C.-L. Tien, J. Heat Transfer **122**, 536 (2000).
[16] Y. F. Chen, D. Y. Li, J. K. Yang, Y. H. Wu, J. R. Lukes, and A. Majumdar, Physica B **349**, 270 (2004).
[17] P. K. Schelling, S. R. Phillpot, and P. Keblinski, Phys. Rev. B **65**, 144306 (2002).
[18] V. Narayanamurti, H. L. Stormer, M. A. Chin, A. C. Gossard, and W. Wiegmann, Phys. Rev. Lett. **43**, 2012 (1979).
[19] S. Mizuno and S. T. Tamura, Phys. Rev. B **45**, 734 (1992).
[20] S. Tamura, D. C. Hurley, and J. P. Wolfe, Phys. Rev. B **38**, 1427 (1988).